Background nitrogen dioxide (NO_2) over the United States and its implications for satellite observations and trends: effects of nitrate photolysis, aircraft, and open fires

Ruijun Dang[1], Daniel J. Jacob[1], Viral Shah[1,a], Sebastian D. Eastham[2,3], Thibaud M. Fritz[2], Loretta J. Mickley[1], Tianjia Liu[4], Yi Wang[5,6], and Jun Wang[5,6]

[1] John A. Paulson School of Engineering and Applied Sciences, Harvard University, Cambridge, MA 02138, USA
[2] Laboratory for Aviation and the Environment, Department of Aeronautics and Astronautics, Massachusetts Institute of Technology, Cambridge, MA 02139, USA
[3] Joint Program on the Science and Policy of Global Change, Massachusetts Institute of Technology, Cambridge, MA 02139, USA
[4] Department of Earth and Planetary Sciences, Harvard University, Cambridge, MA 02138, USA
[5] Center for Global and Regional Environmental Research, Iowa Technology Institute, The University of Iowa, Iowa City, IA 52242, USA
[6] Department of Chemical and Biochemical Engineering, The University of Iowa, Iowa City, IA 52242, USA
[a] Now at Global Modeling and Assimilation Office, NASA Goddard Space Flight Center, Greenbelt, MD 20771, USA, and Science Systems and Applications, Inc., Lanham, MD 20706, USA

Correspondence to: Ruijun Dang (rjdang@seas.harvard.edu)

Abstract. Tropospheric nitrogen dioxide (NO_2) measured from satellites has been widely used to track anthropogenic NO_x emissions, but its retrieval and interpretation can be complicated by the free tropospheric NO_2 background to which satellite measurements are particularly sensitive. Tropospheric NO_2 vertical column densities (VCDs) from the OMI satellite instrument averaged over the contiguous US (CONUS) show no trend after 2009, despite sustained decreases in anthropogenic NO_x emissions, implying an important and rising contribution from the free tropospheric background. Here we use the GEOS-Chem chemical transport model applied to the simulation of OMI NO_2 to better understand the sources and trends of background NO_2 over CONUS. Previous model underestimate of the background is largely corrected by the consideration of aerosol nitrate photolysis, which increases the model NO_2 VCDs by 13% on an annual basis (25% in spring), and also increases the air mass factor (AMF) to convert the tropospheric slant column densities (SCDs) inferred from the OMI spectra into VCDs by 7% on an annual basis (11% in spring). The increase in the AMF decreases the retrieved NO_2 VCDs in the satellite observations, contributing to the improved agreement with the model. Accounting for the 2009-2017 increase in aircraft NO_x emissions drives only a 1.4% mean increase in NO_2 VCDs over CONUS and a 2% increase in the AMF, but the combination of decreasing surface NO_x emissions and increasing aircraft emissions is expected to drive a 14% increase in the AMF over the next decade that will be necessary to account for in the interpretation of satellite NO_2 trends. Fire smoke identification with the NOAA Hazard Mapping System (HMS) indicates that wildfires contribute 1-8% of OMI NO_2 VCDs over the western US

in June-September and that this contribution has been increasing since 2009, contributing to the flattening of OMI NO_2 trends. Future analyses of NO_2 trends from satellite data to infer trends in surface NO_x emissions must critically consider the effects of a rising free tropospheric background due to increasing emissions from aircraft, fires, and possibly lightning.

1 Introduction

Nitrogen oxides ($NO_x \equiv NO + NO_2$) emitted by combustion, lightning, and soils affect oxidant chemistry, air quality, climate, and ecosystems. NO_x cycles chemically to produce tropospheric ozone and is eventually oxidized to nitric acid (HNO_3), which partitions into the particulate phase and is removed by deposition. Satellite observations of tropospheric NO_2 vertical column densities (VCDs) have been used extensively to infer anthropogenic NO_x emissions and their changes (Martin et al., 2003; Boersma et al., 2008; Russell et al., 2012; Duncan et al., 2016; Miyazaki et al., 2017; Matthew J. Cooper et al., 2020; Wang et al., 2020). However, recent studies for North America suggest that the free tropospheric background NO_2 (above ~2 km altitude) could make a large and increasing contribution to the tropospheric NO_2 VCDs measured from space (Silvern et al., 2019; Zhu et al., 2019; Qu et al., 2021; Y. Wang et al., 2021; Jiang et al., 2022). Here we investigate the sources of this NO_2 background over the US and the implications for the retrieval and interpretation of satellite observations.

Tropospheric NO_2 has been measured from space by solar backscatter since 1995 with the GOME instrument (Martin et al., 2002). Current instruments include OMI (2004-) (Krotkov et al., 2016), OMPS (2012-) (Yang et al., 2014), TROPOMI (2017-) (van Geffen et al., 2020; Li et al., 2022), and the geostationary GEMS over East Asia (2020-) (Kim et al., 2020). Tropospheric NO_2 is retrieved in three steps: (1) fit the measured backscattered solar spectrum in and around the NO_2 absorption band (400-470 nm) to infer a slant column density (SCD) along the optical path; (2) subtract the stratospheric contribution from the SCD to obtain the tropospheric SCD; (3) convert the tropospheric SCD to a tropospheric vertical column density (VCD) by dividing by an air mass factor (AMF). The AMF accounts for the photon path between the Sun and the satellite instrument in relation to the vertical distribution of NO_2. It is calculated by convolving altitude-dependent detection sensitivities (scattering weights) computed from a radiative transfer model with a local NO_2 normalized vertical profile (shape factor) provided by an independent chemical transport model (CTM) (Palmer et al., 2001). The detection sensitivity typically increases by a factor of 5 from the surface to the upper troposphere because of atmospheric scattering (Martin et al., 2002; Boersma et al., 2016; M. J. Cooper et al., 2020), so that the tropospheric VCD measurement can be most sensitive to free tropospheric NO_2 even under fairly polluted conditions (Travis et al., 2016). The CTM must then properly represent this free tropospheric NO_2 background. Although cloud-slicing methods have been used to isolate the free tropospheric contribution in satellite NO_2 retrievals, these products have large errors that limit their usefulness (Choi et al., 2014; Belmonte Rivas et al., 2015; Marais et al., 2018; Marais et al., 2021).

The importance of characterizing the free tropospheric NO_2 background was brought to the fore by the use of OMI NO_2 data to infer NO_x emission trends in the contiguous United States (CONUS) (Jiang et al., 2018; Silvern et al., 2019; Qu et al., 2021; Y. Wang et al., 2021; He et al., 2022; Jiang et al., 2022). The OMI NO_2 data over CONUS show a steady decrease from 2005 to 2009 (Russell et al., 2012; Duncan et al., 2013; Duncan et al., 2016; Krotkov et al., 2016), consistent with the decreases of NO_x emissions reported in the EPA National Emission Inventory (NEI), but Jiang et al. (2018) found that the trend flattened after 2009 despite sustained decreases in NO_x emissions according to the NEI and supported by NO_2 surface data (Silvern et al., 2019). This flattening of the trend was attributed by Silvern et al. (2019) to an increasing relative contribution to the OMI NO_2 VCD from the free tropospheric background as the anthropogenic NO_x emissions decrease. Further evidence for this large background contribution emerged from the COVID-19 economic shutdown in 2020 when the response of OMI observations to the decrease of NO_x emissions in CONUS was much less than the response of surface NO_2 observations (Qu et al., 2021). Silvern et al. (2019) pointed out that the post-2009 flattening was most evident for non-urban summer conditions, when background NO_2 would be relatively large, while urban winter conditions showed continued decrease. Y. Wang et al. (2021) explained flattening by an increase in lightning NO_x emissions over the 2009-2019 period, compensating for the sustained decrease in anthropogenic NO_x emissions because of the greater sensitivity of the satellite observations to the free troposphere. Previous studies with the GEOS-Chem CTM underestimated free tropospheric NO_2 over CONUS relative to aircraft observations (Travis et al., 2016; Silvern et al., 2018), but Shah et al. (2023) found that this could reflect in part positive interferences in the aircraft NO_2 measurements, and in part a missing source of free tropospheric NO_x from photolysis of aerosol nitrate.

Aircraft and wildfires could also contribute to the background NO_2 trend but this has not been studied so far. Aircraft emissions increased at a rate of 3.3% per year over the past decade (Lee et al., 2021). Aircraft emission inventories in the CTMs used for satellite retrievals tend to be outdated and do not account for this rapid growth (Boersma et al., 2018; Lamsal et al., 2021). Large NO_2 enhancements have been detected by satellites at fire locations (Mebust et al., 2011; Griffin et al., 2021; Jin et al., 2021), but little is known about the more general contribution of fires to the tropospheric NO_2 background. A recent study reported that 19-56% of peroxyacetyl nitrate (PAN) detected in the free troposphere over the western US in summer 2018 by the Cross-Track Infrared Sounder (CrIS) was associated with fire smoke (Juncosa Calahorrano et al., 2021). Wildfires have become increasingly frequent and intense in the US over the past two decades (Westerling, 2016; Jaffe et al., 2020) and the fire season has lengthened (Cattau et al., 2020), both of which would contribute to an increase in background NO_2.

Here we combine GEOS-Chem simulations and data analysis to better understand the sources and trends of the free tropospheric background NO_2 (and more generally background NO_x) in CONUS by (1) investigating the role of aerosol nitrate photolysis as a source of NO_x (Shah et al., 2023), (2) quantifying the effect of increasing aircraft emissions with the Aircraft Emissions Inventory Code (AEIC; Simone et al., 2013), and (3) quantifying wildfire influence with the NOAA

Hazard Mapping System (HMS) smoke product (Rolph et al., 2009). Increasing NO_2 in the model free troposphere increases the AMF and thus decreases the NO_2 tropospheric VCDs retrieved from satellite. We will see that this significantly improves agreement between GEOS-Chem and OMI observations of NO_2.in different seasons.

2 GEOS-Chem model

We use the GEOS-Chem global CTM version 13.1.2 (https://doi.org/10.5281/zenodo.5014891) driven by MERRA-2 meteorology (Gelaro et al., 2017) in a simulation of oxidant-aerosol chemistry over CONUS in 2009 and 2017. The simulation is at the native MERRA-2 0.5° × 0.625° resolution over North America (10–70° N, 140–40° W), nested in a 4° × 5° global simulation with boundary conditions updated every 3 h. GEOS-Chem 13.1.2 includes a detailed representation of chemistry with recent updates for NO_x uptake by aerosols and clouds (Holmes et al., 2019), isoprene chemistry (Bates and Jacob, 2019), and halogen chemistry (X. Wang et al., 2021). Dry deposition follows a standard resistance-in-series scheme (Wesely, 1989), with HNO_3 updates from Jaeglé et al. (2018). Wet deposition includes in-cloud rainout, below-cloud washout, and scavenging in convective updrafts (Liu et al., 2001). We use a faster washout rate for HNO_3 described in Luo et al. (2019) and previously used in GEOS-Chem simulations over China (Zhai et al., 2021) and the remote oceans (Travis et al., 2020).

Table 1 gives the CONUS NO_x emissions in the model for 2009 and 2017. Global anthropogenic emissions for individual years are from the Community Emissions Data System (CEDS) (McDuffie et al., 2020). This is superseded for the US by the EPA NEI2016 inventory for 2016 (https://www.epa.gov/air-emissions-modeling/2016v1-platform), scaled to 2009 and 2017 using national emission totals (EPA, 2021). Soil NO_x emissions are from Hudman et al. (2012) and updated by Y. Wang et al. (2021) to allow for increased soil NO_x emissions under high temperature conditions (30-40° C) and using soil temperatures from MERRA-2 instead of air temperatures. We reduced the summertime soil NO_x emissions in the midwestern US (38-50° N, 105-95° W) by 50%, as suggested by a previous comparison with OMI NO_2 observations (Vinken et al., 2014). Lightning NO_x emissions are computed following Murray et al. (2012), with lightning flash density spatially constrained by Lightning Imaging Sensor/Optical Transient Detector (LIS/OTD) climatology, interannual variation driven by convective cloud height from MERRA-2, and vertical distribution following Ott et al. (2010). Monthly open fire emissions are taken from the Global Fire Emissions Database version 4 with small fires (GFED4s) (van der Werf et al., 2017), with all releases at the surface. Interannual variations in GFED4s are driven by changes in fuel load, which is a function of meteorology and vegetation type, and burned area and active fire data derived from MODIS satellite observations. Not included in Table 1 is the source from cross-tropopause transport of reactive nitrogen oxides produced in the stratosphere by oxidation of N_2O. This source is included in the model but is negligibly small (0.2 Tg N a^{-1} globally; Bey et al., 2001).

Table 1. Contiguous US (CONUS) NO_x emissions in 2009 and 2017 [Tg N a^{-1}] [a].

	2009	2017
Total	4.9	3.6
Fuel combustion [b]	3.8	2.3
Lightning	0.43	0.48
Soil	0.55	0.60
Aircraft	0.13	0.16
Open fires	0.03	0.10

[a] as used in the GEOS-Chem simulations described in the text.

[b] excluding aircraft.

For aircraft emissions, we use an updated inventory for 2019 produced by the Aircraft Emissions Inventory Code (AEIC) developed at MIT (Simone et al., 2013). It includes daily emissions during both landing and take-off (LTO) and at cruise with horizontal resolution of 0.5° × 0.625° and vertical resolution of 36 layers up to 100 hPa. 81% of these emissions are released above 5 km altitude, and 73% above 8 km. AEIC2019 is scaled to individual years and for different continental regions by using the kerosene consumption data provided by the International Energy Agency (IEA, https://www.iea.org/fuels-and-technologies/oil). The NO_x emission factor increased by 7% from 2005 to 2019 due to increase in combustor temperatures (Dedoussi, 2021; Lee et al., 2021). As shown in Figure 1, aviation NO_x emissions increased globally by 51% from 2005 to 2019, largely driven by rapid growth in developing countries such as China, and by 17% for CONUS. The dip in 2007-2009 is due to the economic recession (Bows-Larkin et al., 2016). AEIC2019 may underestimate aircraft emissions by 10-40% because it does not consider military aircraft, estimated to account for 10-13% of total emissions (Wilkerson et al., 2010) and because it assumes great circle routes which could underestimate emission by up to 28% (Zhang et al., 2022). The effect of aircraft emissions on upper tropospheric NO_x in GEOS-Chem may further be underestimated by 10% due to nonlinear aircraft plume chemistry increasing the NO_x lifetime (Fritz et al., 2020).

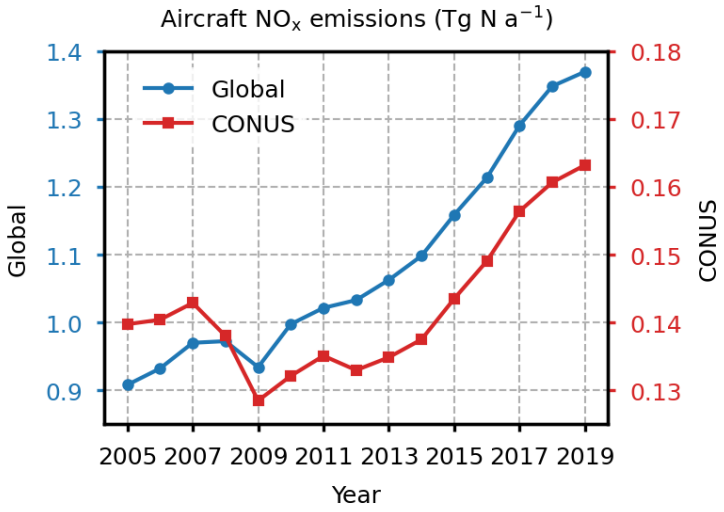

Figure 1: Global and CONUS aircraft NO_x emissions in the AEIC2019 inventory from 2005 to 2019 (Lee et al., 2021).

Table 1 shows a decrease from 2009 to 2017 in fuel combustion emissions (excluding aircraft) but an increase in all other NO_x emissions. The increase in lightning + soil is consistent though somewhat higher than the 6% increase of these sources for 2009-2019 inferred by Y. Wang et al. (2021) from linear regression of the emission time series. Open fire emissions have large interannual variability but are negligibly small in the model; we will use an observation-based analysis in Section 5 for an independent assessment of the contributions of these emissions to satellite NO_2. Overall, we see from Table 1 that CONUS NO_x emissions in the model decreased by 27% from 2009 to 2017, with the 36% decrease in emissions from fuel combustion offset by increases in other emissions. Because these other emissions are more weighted to the free troposphere, they would play a disproportionate role in flattening the OMI NO_2 trend as shown by Y. Wang et al. (2021). They would also effectively increase the AMF in the satellite retrievals, so that the flattening would be exaggerated in the observations if this AMF increase is not accounted for.

We also add in our simulation the photolysis of particulate nitrate (pNO_3^-) previously introduced in GEOS-Chem by Kasibhatla et al. (2018) and Shah et al. (2023) to correct model underestimates of tropospheric NO_x. Gas-phase HNO_3 can be recycled to NO_x through photolysis or reaction with OH, but this process is slow with a lifetime of 15-30 days in the troposphere (Dulitz et al., 2018). pNO_3^- can also be photolyzed at UV wavelengths (>290 nm) and its absorption spectrum peaks around 302 nm (Gen et al., 2022). Previous studies have reported a photolysis rate of pNO_3^- 10-300 times faster than that of HNO_3 (Ye et al., 2016; Reed et al., 2017; Ye et al., 2017), , recycling NO_x through two branches producing NO_2 and nitrous acid (HONO). This process has been found to be an important missing source of NO_x over the remote oceans (Ye et al., 2016; Reed et al., 2017; Kasibhatla et al., 2018; Shah et al., 2023; Andersen et al., 2023). The enhancement factor (EF)

of nitrate photolysis relative to HNO_3 photolysis could be promoted by the coexistence of halides (Wingen et al., 2008; Richards et al., 2011; Zhang et al., 2020) and organic matter (Scharko et al., 2014; Wang et al., 2021), and is further affected by aerosol pH (Scharko et al., 2014) and the nature of cations (Richards et al., 2015).

Shah et al. (2023) found that incorporating aerosol nitrate photolysis in GEOS-Chem largely corrected the model's underestimation of NO_x over the oceans during the ATom aircraft campaign. Here we follow their approach to calculate EF as a function of the molar concentrations of sea salt aerosol [SSA] and nitrate [pNO_3^-]:

$$\mathrm{EF} = 100 \times \max\left(\frac{[\mathrm{SSA}]}{[\mathrm{SSA}]+[\mathrm{pNO_3^-}]}, 0.1\right), \quad (1)$$

The resulting EF values range from 10 in continental air with low SSA to 100 in marine air, and a 2:1 branching ratio for the HONO:NO_2 branches is assumed.

Figure 2 shows the effect of pNO_3^- photolysis as described above on the simulated NO_2 vertical profiles over CONUS. Extensive evaluation of pNO_3^- concentrations in GEOS-Chem including vertical profiles from aircraft is presented in Luo et al. (2019, 2020) and shows no significant bias. We find that photolysis is negligible as a sink of pNO_3^- (~1%; Figure S1) because deposition dominates, and is also negligible as a source of NO_x in the boundary layer (BL) below 2 km altitude because direct NO_x emission dominates. However, pNO_3^- photolysis increases NO_2 concentrations in the free troposphere by about 25% on an annual basis at all altitudes, the stronger radiation in the UT compensating for the lower pNO_3^- concentrations. The largest increase in free tropospheric NO_2 is in spring due to a combination of high pNO_3^- concentrations and strong radiation. The implications for simulation of OMI observations will be discussed in Section 3.

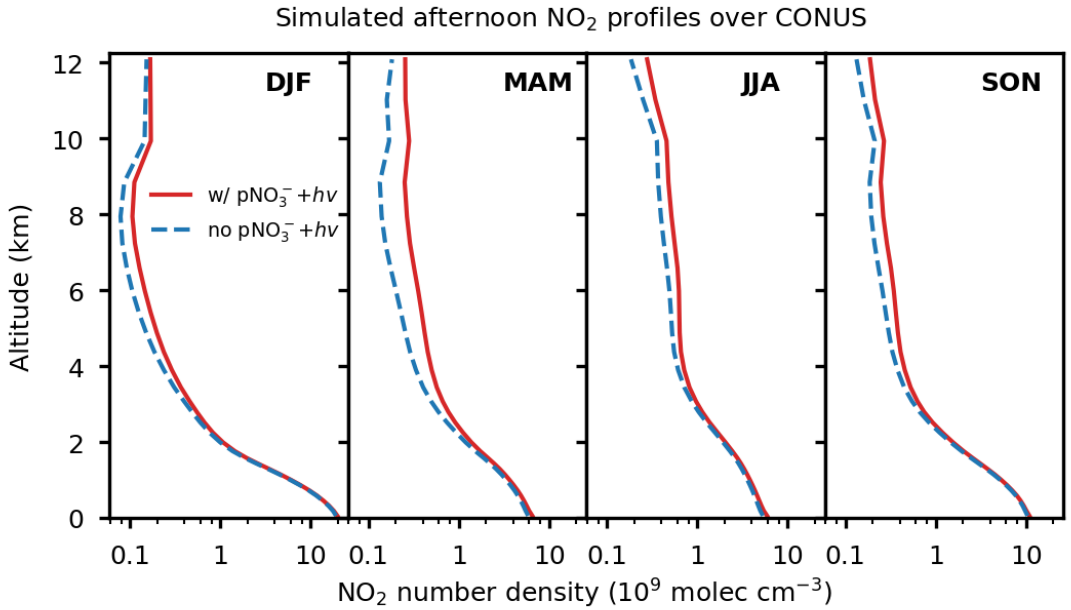

Figure 2: Mean vertical profiles of NO_2 number density simulated by GEOS-Chem over the contiguous US (CONUS) in 2017 at the OMI overpass time of 13-14 local time (LT) and in different seasons. Solid/dashed lines indicate the NO_2 profiles with/without particulate nitrate photolysis ($pNO_3^- + h\nu$). Note log scale for abscissa.

3 Effect of nitrate photolysis on simulation of satellite NO_2 observations

Figure 3 compares OMI observed and GEOS-Chem simulated tropospheric NO_2 VCDs over CONUS in 2017. The OMI instrument onboard the Aura satellite provides daily global coverage at 13:30 local time (LT) with 13×24 km^2 nadir pixel resolution. Here, we use NO_2 retrievals from version 4.0 of the NASA OMI NO_2 level 2 product (OMNO2; https://disc.gsfc.nasa.gov/datasets/OMNO2_003/summary) (Lamsal et al., 2021), filtered by removing pixels with cloud fraction >0.2, surface reflectivity >0.3, solar zenith angle >75°, view zenith angle >65°, as well as pixels affected by the so-called row anomaly (Dobber et al., 2008). The $OMNO_2$ product uses vertical shape factors from the Global Modeling Initiative (GMI) CTM in its AMF calculation. To conduct a consistent comparison with GEOS-Chem, we recompute the AMFs and hence the OMI retrievals (now referred to as OMI-GC) using local GEOS-Chem NO_2 shape factors sampled at 13-14 LT (Boersma et al., 2016; M. J. Cooper et al., 2020).

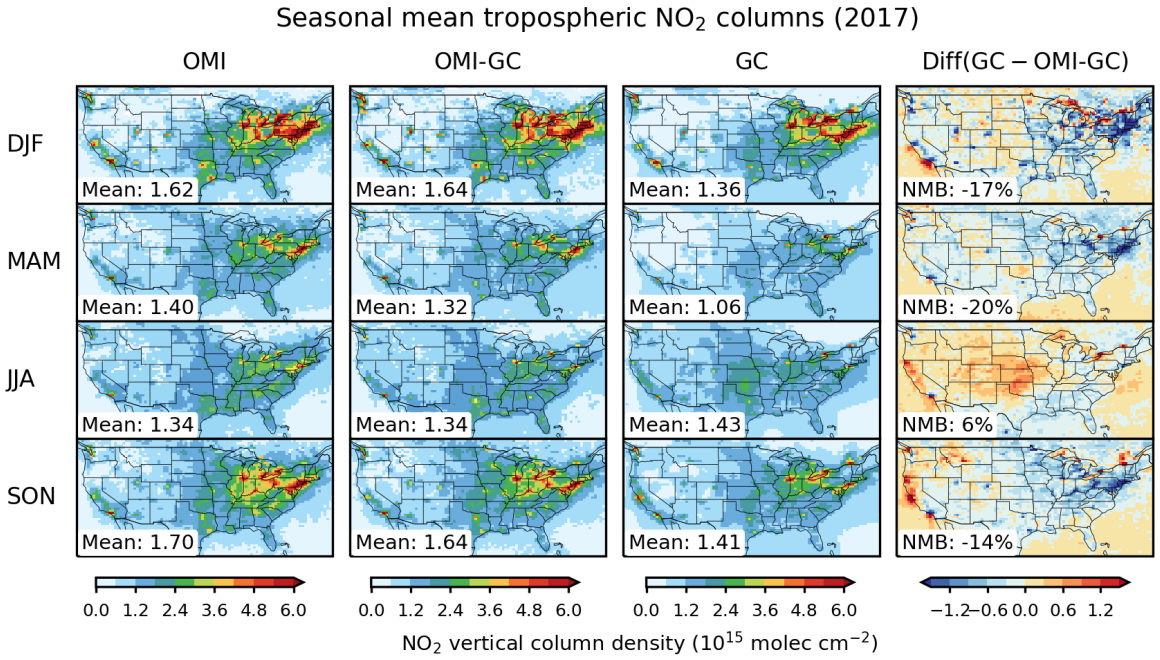

Figure 3: Seasonal mean tropospheric NO_2 vertical column densities (VCDs) over CONUS in 2017. From left to right are the $OMNO_2$ OMI retrievals with AMFs computed using the GMI NO_2 vertical profiles (OMI), the OMI retrievals with AMFs computed using the GEOS-Chem NO_2 vertical profiles (OMI-GC), the GEOS-Chem simulation (GC), and the difference between GC and OMI-GC. Mean values over CONUS and normalized mean bias (NMB) between GC and OMI-GC are given inset.

GEOS-Chem generally captures the observed spatial distribution and seasonal variation of tropospheric NO_2 VCDs in CONUS. The normalized mean bias (NMB) is -17% in winter, -20% in spring, +6% in summer, and -14% in fall. In comparison, the NMB without nitrate photolysis is -24% in winter, -43% in spring, -14% in summer, and -26% in fall. Adding nitrate photolysis greatly improves the agreement, and its effect on NO_2 VCDs and AMFs in 2017 is shown in Figure 4. It increases simulated tropospheric NO_2 VCDs by 13% over CONUS, with the largest increase in spring (25%). In figure 4b, we calculate the monthly AMFs by using scattering weights from OMNO2 v4 and GEOS-Chem NO_2 shape factors with and without nitrate photolysis to determine the effect of nitrate photolysis on NO_2 retrievals. Annual mean AMF increases by 7% and spring AMF increases by 11% with nitrate photolysis because the shape factor is shifted to higher altitudes (Figure 2). As a result, the NO_2 VCDs retrieved using the GEOS-Chem NO_2 shape factor (OMI-GC) with nitrate photolysis is 7% lower than that retrieved using the shape factor without nitrate photolysis (Figure 4a), and this further improves agreement with the model simulation. The annual mean AMF using the GEOS-Chem shape factor with nitrate photolysis is now 1.21, closer to the AMF calculated using the GMI shape factor (1.19). GMI does not include nitrate

photolysis but has slower NO_x loss from N_2O_5 chemistry than GEOS-Chem (Shah et al., 2023). Better agreement is also found in year 2009 between simulated and retrieved tropospheric NO_2 VCDs with the addition of nitrate photolysis (Figure S2). The NMB improves from -8% to 1% and the corresponding AMFs increases by 3%. The nitrate photolysis effect is smaller in 2009 than in 2017, mostly because of larger surface anthropogenic emissions increasing NO_2 in the PBL relative to the free troposphere. Previous studies found that GEOS-Chem could not fully reproduce the flattening of the NO_2 trend over CONUS seen by OMI (Silvern et al., 2019; Qu et al., 2021; left panel of Figure 5). Inclusion of nitrate photolysis significantly corrects the discrepancy, reducing by 45% the difference between modeled and retrieved changes over the 2009-2017 period (right panel of Figure 5).

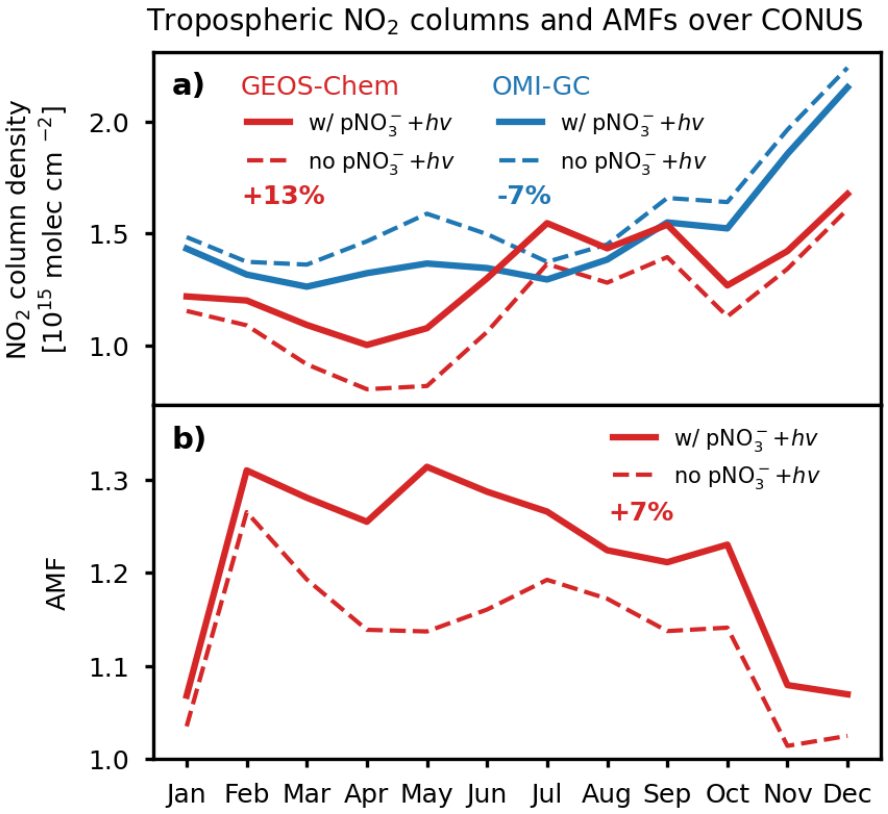

Figure 4: Sensitivity to particulate nitrate photolysis of tropospheric NO_2 vertical column densities (VCDs) simulated by GEOS-Chem and retrieved from OMI satellite observations over CONUS. The top panel shows 2017 monthly mean GEOS-Chem NO_2 VCDs with and without nitrate photolysis, and the OMI retrieval using GEOS-Chem shape factors (OMI-GC) with and without nitrate photolysis. The bottom panel shows the monthly mean air mass factor (AMF) for OMI tropospheric NO_2 retrievals with and without nitrate photolysis. Numbers inset give annual mean percentage differences for the different quantities with versus without nitrate photolysis.

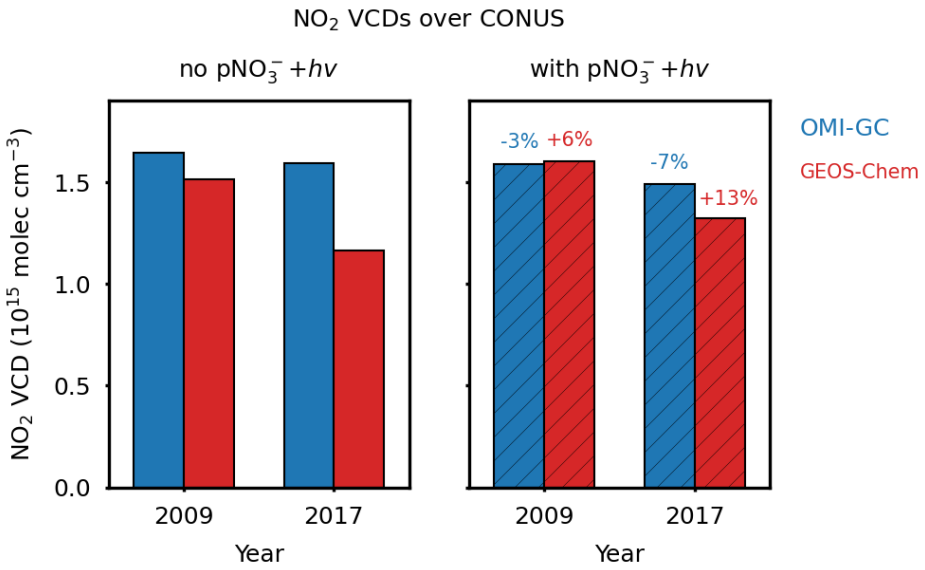

Figure 5. Changes in NO_2 vertical column densities (VCDs) over the contiguous United States (CONUS) between 2009 and 2017 as observed by OMI (OMI-GC) and simulated by GEOS-Chem. Values are annual means averaged spatially over CONUS. The OMI-GC retrievals use GEOS-Chem vertical shape factors and are therefore sensitive to the relative vertical distribution of NO_2 simulated by GEOS-Chem. The left panel shows results for the standard GEOS-Chem simulation without particulate nitrate photolysis, and the right panel shows results from the simulation with particulate nitrate photolysis. The percent changes resulting from the addition of particulate nitrate photolysis are indicated on top of each bar.

Overall, our GEOS-Chem simulation including pNO_3^- photolysis is consistent with the OMI observations within their 35% estimated uncertainty (Lamsal et al., 2021), reflecting the combined and opposite effects of pNO_3^- photolysis on the simulated NO_2 VCDs and on the satellite retrieval. Figure 3 still shows some regional discrepancies between GEOS-Chem and OMI. Low biases are found in urban areas that may reflect biases in model chemistry at 50 km resolution but also bias in the satellite NO_2 retrievals (Laughner and Cohen, 2019; Laughner et al., 2019). There is a high bias in the central US during the summer, even before the inclusion of nitrate photolysis, partly due to the use of the updated soil NO_x scheme of Y. Wang et al. (2021) in GEOS-Chem that increases emissions at high temperatures 021). On the west coast, high biases are found in fire-influenced areas but that may be due to OMI retrievals being too low. Most current operational NO_2 retrieval algorithms including OMNO2 v4 treat aerosols implicitly (Liu et al., 2020; Vasilkov et al., 2021), resulting in low retrieved NO_2 in fire plumes (Griffin et al., 2021). Travis et al. (2016) previously found a 30% GEOS-Chem overestimate of the NASA OMI NO_2 v2.1 retrieval over the Southeast US in summer, which they attributed to the NEI2011 emissions being too high, but that

model bias is largely corrected in our simulation due both to downward revision of NO_x emissions in NEI2016 and to 10-40% higher OMI NO_2 retrievals in version 4 of OMNO2 relative to previous versions (Lamsal et al., 2021).

4 Effect of aircraft emissions and future AMF projections

We isolated the effect of the 2009-2017 increase in aircraft emissions (Fig. 1) on NO_2 VCDs and AMFs over CONUS by conducting sensitivity simulations with the AEIC emission trends but with all other conditions fixed for 2017 including anthropogenic surface emissions. The increase in aircraft emissions since 2009 leads to a 1.4% increase in the simulated annual mean tropospheric NO_2 VCDs over CONUS, with 75% of the increase above 6 km. The AMF increases by 1.7% as the vertical distribution of NO_2 shifts from the boundary layer to the upper troposphere. This influence from aircraft emissions is expected to increase in the future, as shown in Figure 6 with a projection to 2032. In this projection, anthropogenic emissions over CONUS are assumed to continue to decrease at the current rate of 5.9% a^{-1}. Global aircraft emissions are 20% lower in 2022 than in 2019 due to the pandemic. We assume they return to 2019 levels in 2023, and increase at a rate of 3.6% a^{-1} in the following decade (Airbus, 2022; Boeing, 2022). We calculate the resulting AMFs by applying scattering weights from OMNO2 v4 to the extrapolated NO_2 vertical profiles and find an AMF increase of 20% over the 2017-2032 period, including 80% from decrease in surface emissions and 20% from increase in aircraft emissions. Increasing aircraft emissions will likely play an increasing role in increasing the AMF in the future.

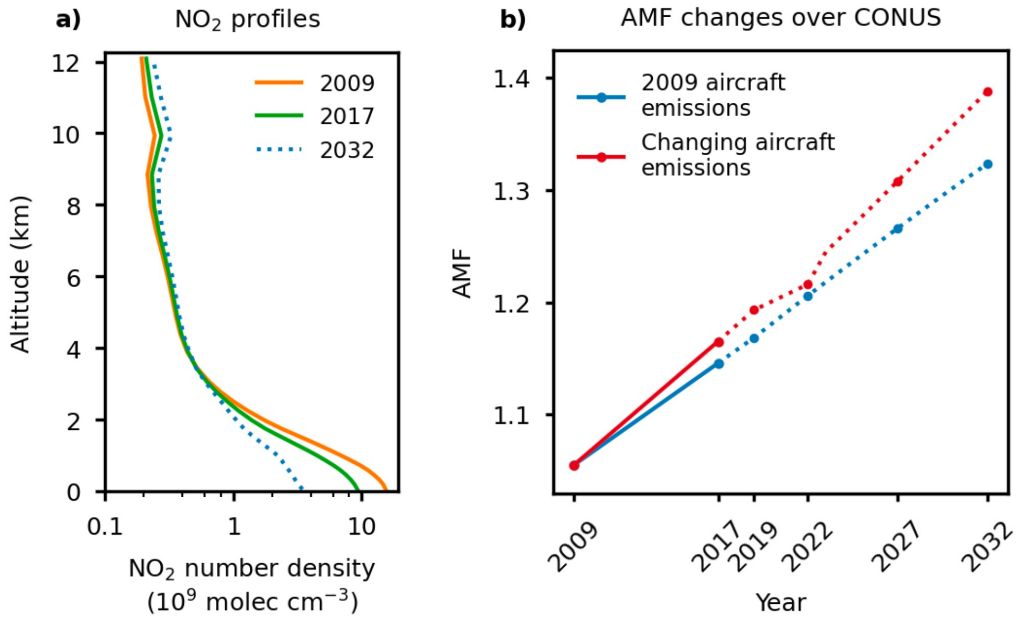

Figure 6: Effect of changing surface anthropogenic and aircraft emissions on tropospheric NO_2 vertical profiles and air mass factors (AMFs) for satellite retrievals over the 2009-2032 period. a) Mean NO_2 afternoon profiles over CONUS in 2009,

2017, and 2032 (projected), accounting for changes in surface and aircraft emissions. b) AMFs for tropospheric NO_2 retrievals over CONUS from 2009 to 2032, with the red line calculated using NO_2 profiles with reduced anthropogenic surface emissions and increased aircraft emissions, and the blue line with reduced anthropogenic surface emissions only and fixed aircraft emissions for 2009. Solid lines are from GEOS-Chem simulations for 2009 and 2017, while dashed lines scale the 2009-2017 NO_2 simulation differences to the projected changes in emissions beyond 2017.

5 Effect of open fire emissions

Open fire emissions make a very small contribution to the mean CONUS NO_x budget in GEOS-Chem (Table 1), but they could be of seasonal importance in the western US in June-September (Jaffe et al., 2020). Simulation of fire NO_x in models such as GEOS-Chem is affected by uncertainties not only in emissions (Carter et al., 2020) but also in plume lofting and chemistry (Zhu et al., 2018; Palm et al., 2021; Peng et al., 2021). Interpreting fire NO_2 observations by satellites is complicated by scattering and absorption from the smoke aerosols (Castellanos et al., 2015; Griffin et al., 2021) as well as plume lofting (Jin et al., 2021) and any differences in vertical distribution between NO_2 and the smoke aerosols.

Here we use the Hazard Mapping System (HMS) product (Rolph et al., 2009) from the National Oceanic and Atmospheric Administration (NOAA) to identify fire-impacted OMI retrievals and estimate from there the contribution of fire to NO_2 VCDs as observed by OMI. HMS provides daily daytime locations and extent of smoke plumes as determined by human analysts using satellite imagery to delineate smoke-affected areas. The dataset has been widely used to identify such areas (Brey and Fischer, 2016; Fischer et al., 2018; Juncosa Calahorrano et al., 2021). We use the fire-season (June-September) HMS data from 2009 to 2020 (https://www.ospo.noaa.gov/Products/land/hms.html#data) and grid it to a horizontal resolution of 0.25°x0.25°. For each grid cell, we define days associated with smoke plumes in the HMS data as fire-affected days and the remaining days as fire-free days. Fire-free days may still have some influence of aged fire emissions such as through PAN decomposition, so the distinction offered by the HMS data is for relatively fresh fire emissions over a few days. We thus infer the contribution of fresh fire emissions to the NO_2 VCDs from the difference between the seasonal mean NO_2 VCDs and the average NO_2 VCDs for fire-free days. Previous studies have found that the implicit correction for aerosols in current NO_2 retrieval algorithms as effective clouds could introduce low biases of up to 50% in the retrieved NO_2 VCD in areas of high aerosol loading, such as fire plumes (Lorente et al., 2017; Liu et al., 2020). Therefore, we also examine the effect of increasing tropospheric NO_2 VCDs on fire-affected days by 50%.

Figure 7 shows the contribution of fresh fire emissions to the OMI observations over the western US (130°-114° W, 30°-50° N) and the rest of CONUS in June-September 2009-2020. The red envelope shows the effect of increasing tropospheric NO_2 VCDs on fire-affected days by 50% to account for aerosol-induced bias, and this defines the upper range of fire influence. We find that fires contribute 1-8% (upper range 1-15%) to the OMI NO_2 VCDs over the western US in June-September of

individual years, with a maximum contribution in 2020 which was a particularly high fire year. The fire contribution in the rest of CONUS is negligible. In the absence of fires, we see from Figure 6 that OMI NO_2 over the western US would have significantly decreased over the 2009-2020 period. Increasing fire activity over the past decade contributed to the flattening of the OMI trend. We see no such effect over the rest of CONUS, where open fires have negligible influence, and increasing lightning could be mostly responsible for the flattening of OMI NO_2 there (Y. Wang et al., 2021).

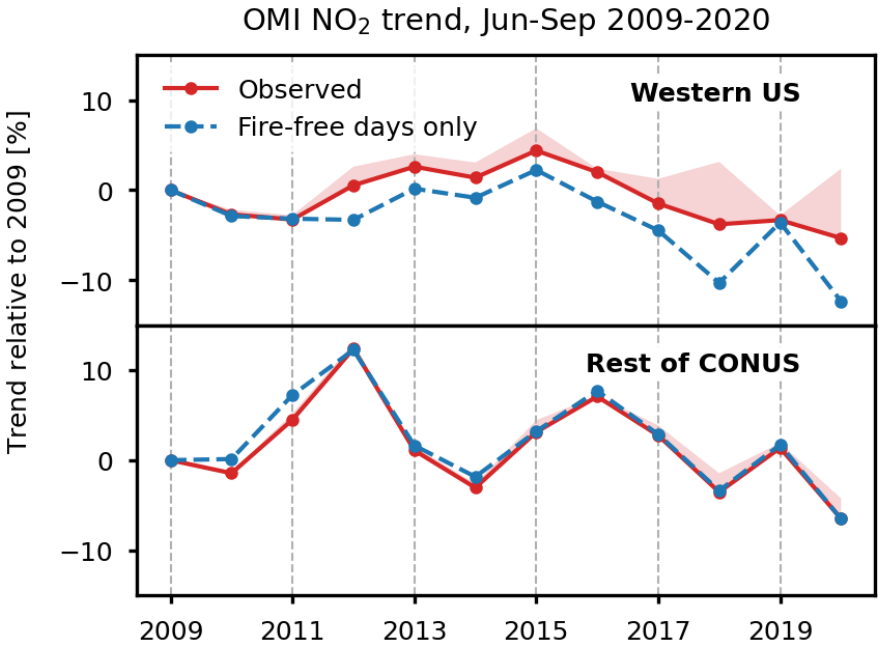

Figure 7: Trends of OMI tropospheric NO_2 VCDs over the western US and the rest of CONUS for June-September 2009-2020, examining the effects of fires. Trends are shown relative to 2009. The overall trend from the OMI observations (OMNO2 retrieval) is shown in red, and the trend for the subset of fire-free days is shown as dashed. Fire-free days are identified from the NOAA HMS product (see text). The red envelope shows the effect of a 50% bias correction of the OMI NO_2 retrieval on fire-affected days. The western US domain is defined as (130°-114° W, 30°-50° N).

6 Conclusions

OMI satellite observations of tropospheric NO_2 vertical column densities (VCDs) over the contiguous US (CONUS) show a flattening trend after 2009 despite continuous decrease in surface anthropogenic NO_x emissions. This suggests a large and rising contribution from background NO_2 in the free troposphere (above 2 km) to the tropospheric NO_2 VCDs observed from space, but previous simulations with the GEOS-Chem chemical transport model have been unable to account for this

background. Here, we used the GEOS-Chem chemical transport model including a new mechanism for particulate nitrate photolysis and the AEIC2019 inventory for aircraft emission trends, together with the NOAA Hazard Mapping System (HMS) smoke product, to better understand the magnitude and trends of free tropospheric background NO_2 and the implications for retrieval and interpretation of satellite data.

Inclusion of particulate nitrate photolysis as a secondary source of NO_x in GEOS-Chem, following recent field and laboratory evidence, increases the annual mean tropospheric NO_2 VCDs over CONUS by 13% with the maximum effect in spring (25%). It also increases the air mass factor (AMF) for the satellite tropospheric NO_2 retrieval by 7% on an annual basis (11% in spring) because of the increased contribution of the free troposphere to the tropospheric NO_2 VCD. The combination of these two effects provides an improved fit of GEOS-Chem to the OMI satellite NO_2 data, particularly in the spring when the model underestimate was worst. The consideration of nitrate photolysis in 2009 and 2017 corrects 45% of the discrepancy between GEOS-Chem and OMI NO_2 changes over that period, because it increases the free tropospheric contribution to the NO_2 VCDs while the surface anthropogenic emissions decline.

Aircraft NO_x emissions increased by 38% globally from 2009 to 2017 and by 20% over CONUS but this has generally not been taken into account in the models used to derive vertical shape factors for satellite NO_2 retrievals. The associated increase in the annual mean AMF is only 2% because aircraft emissions remain relatively low compared to lightning. Sustained increases in aircraft emissions in the future, combined with sustained decreases in surface anthropogenic emissions, are expected to increase the AMF by 14% over the next decade with major implications for interpretation of NO_2 trends from satellite data.

The contribution of open fires to the free tropospheric NO_2 background is difficult to diagnose in GEOS-Chem due to uncertainties in plume lofting and chemistry. Instead, we used the NOAA Hazard Mapping System (HMS) to separate fire-free from fire-affected days in the OMI NO_2 data during the June-September fire season in the western US. We find that fires contribute only 1-8% of the seasonal OMI NO_2 in that region for individual years, but with an increasing trend over 2009-2017 that could offset the decrease in anthropogenic emissions and contribute to the flattening of the OMI NO_2 tropospheric VCD trend during that period.

Our work demonstrates the importance of properly accounting for the free tropospheric background in interpreting NO_2 observations from space. Better understanding is needed of the role of aerosol nitrate photolysis, which remains highly uncertain. Increasing contributions to the tropospheric NO_2 VCD from free tropospheric sources including aircraft and fires, combined with decrease in surface anthropogenic emissions, will be critical to consider in future analyses of NO_2 trends from satellite data.

Data availability

The OMNO2 product are available at https://disc.gsfc.nasa.gov/datasets/OMNO2_003/summary. The HMS data can be downloaded from https://www.ospo.noaa.gov/Products/land/hms.html#data.The AEIC2019 inventory is now in the default GEOS-Chem version13.4. All other model results are available on request from the corresponding author.

Author contributions

DJJ and RD designed the study. RD conducted model simulations and analyzed satellite and model data. VS contributed nitrate photolysis in GEOS-Chem and supported data analysis. SDE and FT provided aircraft emission inventory and supporting guidance. JW and YW contributed soil NO_x emission scheme in GEOS-Chem. LJM and TL helped with interpretation and discussion related to HMS product. RD and DJJ wrote the manuscript and all authors contributed to the revision of the paper.

Competing interests

The authors declare that they have no conflict of interest.

Acknowledgements

We acknowledge the Global Modeling and Assimilation Office (GMAO) at NASA Goddard Space Flight Center for providing the MERRA-2 data.

Financial support

This work was supported by the NASA Aura Science Team and by the US EPA Science to Achieve Results (STAR) Program.

References

Global Market Forecast 2022−2041: https://www.airbus.com/en/products-services/commercial-aircraft/market/global-market-forecast, 2022.

Andersen, S. T., Carpenter, L. J., Reed, C., Lee, J. D., Chance, R., Sherwen, T., Vaughan, A. R., Stewart, J., Edwards, P. M., Bloss, W. J., Sommariva, R., Crilley, L. R., Nott, G. J., Neves, L., Read, K., Heard, D. E., Seakins, P. W., Whalley, L. K., Boustead, G. A., Fleming, L. T., Stone, D., and Fomba, K. W.: Extensive field evidence for the release of HONO from the photolysis of nitrate aerosols, Sci. Adv., 9, eadd6266, doi:10.1126/sciadv.add6266, 2023.

Bates, K. H., and Jacob, D. J.: A new model mechanism for atmospheric oxidation of isoprene: global effects on oxidants, nitrogen oxides, organic products, and secondary organic aerosol, Atmos. Chem. Phys., 19, 9613-9640, 10.5194/acp-19-9613-2019, 2019.

Belmonte Rivas, M., Veefkind, P., Eskes, H., and Levelt, P.: OMI tropospheric NO₂ profiles from cloud slicing: constraints on surface emissions, convective transport and lightning NO_x, Atmos. Chem. Phys., 15, 13519-13553, 10.5194/acp-15-13519-2015, 2015.

Boeing Commercial Market Outlook 2022-2041: https://www.boeing.com/commercial/market/commercial-market-outlook/, 2022.

Boersma, K. F., Jacob, D. J., Bucsela, E. J., Perring, A. E., Dirksen, R., van der A, R. J., Yantosca, R. M., Park, R. J., Wenig, M. O., Bertram, T. H., and Cohen, R. C.: Validation of OMI tropospheric NO2 observations during INTEX-B and application to constrain NOx emissions over the eastern United States and Mexico, Atmos. Environ., 42, 4480-4497, https://doi.org/10.1016/j.atmosenv.2008.02.004, 2008.

Boersma, K. F., Vinken, G. C. M., and Eskes, H. J.: Representativeness errors in comparing chemistry transport and chemistry climate models with satellite UV–Vis tropospheric column retrievals, Geosci. Model Dev., 9, 875-898, 10.5194/gmd-9-875-2016, 2016.

Boersma, K. F., Eskes, H. J., Richter, A., De Smedt, I., Lorente, A., Beirle, S., van Geffen, J. H. G. M., Zara, M., Peters, E., Van Roozendael, M., Wagner, T., Maasakkers, J. D., van der A, R. J., Nightingale, J., De Rudder, A., Irie, H., Pinardi, G., Lambert, J. C., and Compernolle, S. C.: Improving algorithms and uncertainty estimates for satellite NO2 retrievals: results from the quality assurance for the essential climate variables (QA4ECV) project, Atmos. Meas. Tech., 11, 6651-6678, 10.5194/amt-11-6651-2018, 2018.

Bows-Larkin, A., Mander, S. L., Traut, M. B., Anderson, K. L., and Wood, F. R.: Aviation and Climate Change–The Continuing Challenge, in: Encyclopedia of Aerospace Engineering, 1-11, 2016.

Brey, S. J., and Fischer, E. V.: Smoke in the City: How Often and Where Does Smoke Impact Summertime Ozone in the United States?, Environ. Sci. Technol., 50, 1288-1294, 10.1021/acs.est.5b05218, 2016.

Carter, T. S., Heald, C. L., Jimenez, J. L., Campuzano-Jost, P., Kondo, Y., Moteki, N., Schwarz, J. P., Wiedinmyer, C., Darmenov, A. S., da Silva, A. M., and Kaiser, J. W.: How emissions uncertainty influences the distribution and radiative impacts of smoke from fires in North America, Atmos. Chem. Phys., 20, 2073-2097, 10.5194/acp-20-2073-2020, 2020.

Castellanos, P., Boersma, K. F., Torres, O., and de Haan, J. F.: OMI tropospheric NO2 air mass factors over South America: effects of biomass burning aerosols, Atmos. Meas. Tech., 8, 3831-3849, 10.5194/amt-8-3831-2015, 2015.

Cattau, M. E., Wessman, C., Mahood, A., and Balch, J. K.: Anthropogenic and lightning-started fires are becoming larger and more frequent over a longer season length in the U.S.A, Global Ecology and Biogeography, 29, 668-681, https://doi.org/10.1111/geb.13058, 2020.

Choi, S., Joiner, J., Choi, Y., Duncan, B. N., Vasilkov, A., Krotkov, N., and Bucsela, E.: First estimates of global free-tropospheric NO2 abundances derived using a cloud-slicing technique applied to satellite observations from the Aura Ozone Monitoring Instrument (OMI), Atmos. Chem. Phys., 14, 10565-10588, 10.5194/acp-14-10565-2014, 2014.

Cooper, M. J., Martin, R. V., Henze, D. K., and Jones, D. B. A.: Effects of a priori profile shape assumptions on comparisons between satellite NO2 columns and model simulations, Atmos. Chem. Phys., 20, 7231-7241, 10.5194/acp-20-7231-2020, 2020.

Cooper, M. J., Martin, R. V., McLinden, C. A., and Brook, J. R.: Inferring ground-level nitrogen dioxide concentrations at fine spatial resolution applied to the TROPOMI satellite instrument, Environ. Res. Lett., 15, 104013, 10.1088/1748-9326/aba3a5, 2020.

Dedoussi, I. C.: Implications of future atmospheric composition in decision-making for sustainable aviation, Environ. Res. Lett., 16, 031002, 10.1088/1748-9326/abe74d, 2021.

Dobber, M., Voors, R., Dirksen, R., Kleipool, Q., and Levelt, P.: The High-Resolution Solar Reference Spectrum between 250 and 550 nm and its Application to Measurements with the Ozone Monitoring Instrument, Solar Physics, 249, 281-291, 10.1007/s11207-008-9187-7, 2008.

Dulitz, K., Amedro, D., Dillon, T. J., Pozzer, A., and Crowley, J. N.: Temperature-(208–318 K) and pressure-(18–696 Torr) dependent rate coefficients for the reaction between OH and HNO3, Atmos. Chem. Phys., 18, 2381-2394, 10.5194/acp-18-2381-2018, 2018.

Duncan, B. N., Yoshida, Y., de Foy, B., Lamsal, L. N., Streets, D. G., Lu, Z., Pickering, K. E., and Krotkov, N. A.: The observed response of Ozone Monitoring Instrument (OMI) NO2 columns to NOx emission controls on power plants in the United States: 2005–2011, Atmos. Environ., 81, 102-111, https://doi.org/10.1016/j.atmosenv.2013.08.068, 2013.

Duncan, B. N., Lamsal, L. N., Thompson, A. M., Yoshida, Y., Lu, Z., Streets, D. G., Hurwitz, M. M., and Pickering, K. E.: A space-based, high-resolution view of notable changes in urban NOx pollution around the world (2005–2014), Journal of Geophysical Research: Atmospheres, 121, 976-996, https://doi.org/10.1002/2015JD024121, 2016.

EPA: Annual Average Emissions, Air Pollutant Emission Trends Data: https://www.epa.gov/air-emissions-inventories/air-pollutant-emissions-trends-data, 2021.

Fischer, E. V., Zhu, L., Payne, V. H., Worden, J. R., Jiang, Z., Kulawik, S. S., Brey, S., Hecobian, A., Gombos, D., Cady-Pereira, K., and Flocke, F.: Using TES retrievals to investigate PAN in North American biomass burning plumes, Atmos. Chem. Phys., 18, 5639-5653, 10.5194/acp-18-5639-2018, 2018.

Gelaro, R., McCarty, W., Suarez, M. J., Todling, R., Molod, A., Takacs, L., Randles, C. A., Darmenov, A., Bosilovich, M. G., Reichle, R., Wargan, K., Coy, L., Cullather, R., Draper, C., Akella, S., Buchard, V., Conaty, A., da Silva, A. M., Gu, W., Kim, G. K., Koster, R., Lucchesi, R., Merkova, D., Nielsen, J. E., Partyka, G., Pawson, S., Putman, W., Rienecker, M., Schubert, S. D., Sienkiewicz, M., and Zhao, B.: The Modern-Era Retrospective Analysis for Research and Applications, Version 2 (MERRA-2), J. Clim., 30, 5419-5454, 10.1175/jcli-d-16-0758.1, 2017.

Gen, M., Liang, Z., Zhang, R., Go Mabato, B. R., and Chan, C. K.: Particulate nitrate photolysis in the atmosphere, Environmental Science: Atmospheres, 2, 111-127, 10.1039/D1EA00087J, 2022.

Griffin, D., McLinden, C. A., Dammers, E., Adams, C., Stockwell, C. E., Warneke, C., Bourgeois, I., Peischl, J., Ryerson, T. B., Zarzana, K. J., Rowe, J. P., Volkamer, R., Knote, C., Kille, N., Koenig, T. K., Lee, C. F., Rollins, D., Rickly, P. S., Chen, J., Fehr, L., Bourassa, A., Degenstein, D., Hayden, K., Mihele, C., Wren, S. N., Liggio, J., Akingunola, A., and Makar, P.: Biomass burning nitrogen dioxide emissions derived from space with TROPOMI: methodology and validation, Atmos. Meas. Tech., 14, 7929-7957, 10.5194/amt-14-7929-2021, 2021.

He, T.-L., Jones, D. B. A., Miyazaki, K., Huang, B., Liu, Y., Jiang, Z., White, E. C., Worden, H. M., and Worden, J. R.: Deep Learning to Evaluate US NOx Emissions Using Surface Ozone Predictions, Journal of Geophysical Research: Atmospheres, 127, e2021JD035597, https://doi.org/10.1029/2021JD035597, 2022.

Holmes, C. D., Bertram, T. H., Confer, K. L., Graham, K. A., Ronan, A. C., Wirks, C. K., and Shah, V.: The Role of Clouds in the Tropospheric NOx Cycle: A New Modeling Approach for Cloud Chemistry and Its Global Implications, Geophysical Research Letters, 46, 4980-4990, https://doi.org/10.1029/2019GL081990, 2019.

Hudman, R. C., Moore, N. E., Mebust, A. K., Martin, R. V., Russell, A. R., Valin, L. C., and Cohen, R. C.: Steps towards a mechanistic model of global soil nitric oxide emissions: implementation and space based-constraints, Atmospheric Chemistry and Physics, 12, 7779-7795, 10.5194/acp-12-7779-2012, 2012.

Jaeglé, L., Shah, V., Thornton, J. A., Lopez-Hilfiker, F. D., Lee, B. H., McDuffie, E. E., Fibiger, D., Brown, S. S., Veres, P., Sparks, T. L., Ebben, C. J., Wooldridge, P. J., Kenagy, H. S., Cohen, R. C., Weinheimer, A. J., Campos, T. L., Montzka, D. D., Digangi, J. P., Wolfe, G. M., Hanisco, T., Schroder, J. C., Campuzano-Jost, P., Day, D. A., Jimenez, J. L., Sullivan, A. P., Guo, H., and Weber, R. J.: Nitrogen Oxides Emissions, Chemistry, Deposition, and Export Over the Northeast United States During the WINTER Aircraft Campaign, Journal of Geophysical Research: Atmospheres, 123, 12,368-312,393, https://doi.org/10.1029/2018JD029133, 2018.

Jaffe, D. A., O'Neill, S. M., Larkin, N. K., Holder, A. L., Peterson, D. L., Halofsky, J. E., and Rappold, A. G.: Wildfire and prescribed burning impacts on air quality in the United States, J. Air Waste Manage. Assoc., 70, 583-615, 10.1080/10962247.2020.1749731, 2020.

Jiang, Z., McDonald Brian, C., Worden, H., Worden John, R., Miyazaki, K., Qu, Z., Henze Daven, K., Jones Dylan, B. A., Arellano Avelino, F., Fischer Emily, V., Zhu, L., and Boersma, K. F.: Unexpected slowdown of US pollutant emission reduction in the past decade, Proceedings of the National Academy of Sciences, 115, 5099-5104, 10.1073/pnas.1801191115, 2018.

Jiang, Z., Zhu, R., Miyazaki, K., McDonald, B. C., Klimont, Z., Zheng, B., Boersma, K. F., Zhang, Q., Worden, H., Worden, J. R., Henze, D. K., Jones, D. B. A., Denier van der Gon, H. A. C., and Eskes, H.: Decadal Variabilities in Tropospheric Nitrogen Oxides Over United States, Europe, and China, Journal of Geophysical Research: Atmospheres, 127, e2021JD035872, https://doi.org/10.1029/2021JD035872, 2022.

Jin, X., Zhu, Q., and Cohen, R. C.: Direct estimates of biomass burning NOx emissions and lifetimes using daily observations from TROPOMI, Atmos. Chem. Phys., 21, 15569-15587, 10.5194/acp-21-15569-2021, 2021.

Juncosa Calahorrano, J. F., Payne, V. H., Kulawik, S., Ford, B., Flocke, F., Campos, T., and Fischer, E. V.: Evolution of Acyl Peroxynitrates (PANs) in Wildfire Smoke Plumes Detected by the Cross-Track Infrared Sounder (CrIS) Over the Western U.S. During Summer 2018, Geophys. Res. Lett., 48, e2021GL093405, https://doi.org/10.1029/2021GL093405, 2021.

Kasibhatla, P., Sherwen, T., Evans, M. J., Carpenter, L. J., Reed, C., Alexander, B., Chen, Q., Sulprizio, M. P., Lee, J. D., Read, K. A., Bloss, W., Crilley, L. R., Keene, W. C., Pszenny, A. A. P., and Hodzic, A.: Global impact of nitrate photolysis in sea-salt aerosol on NOx, OH, and O3 in the marine boundary layer, Atmos. Chem. Phys., 18, 11185-11203, 10.5194/acp-18-11185-2018, 2018.

Kim, J., Jeong, U., Ahn, M.-H., Kim, J. H., Park, R. J., Lee, H., Song, C. H., Choi, Y.-S., Lee, K.-H., Yoo, J.-M., Jeong, M.-J., Park, S. K., Lee, K.-M., Song, C.-K., Kim, S.-W., Kim, Y. J., Kim, S.-W., Kim, M., Go, S., Liu, X., Chance, K., Chan Miller, C., Al-Saadi, J., Veihelmann, B., Bhartia, P. K., Torres, O., Abad, G. G., Haffner, D. P., Ko, D. H., Lee, S. H., Woo, J.-H., Chong, H., Park, S. S., Nicks, D., Choi, W. J., Moon, K.-J., Cho, A., Yoon, J., Kim, S.-k., Hong, H., Lee, K., Lee, H., Lee, S., Choi, M., Veefkind, P., Levelt, P. F., Edwards, D. P., Kang, M., Eo, M., Bak, J., Baek, K., Kwon, H.-A., Yang, J., Park, J., Han, K. M., Kim, B.-R., Shin, H.-W., Choi, H., Lee, E., Chong, J., Cha, Y., Koo, J.-H., Irie, H., Hayashida, S., Kasai, Y., Kanaya, Y., Liu, C., Lin, J., Crawford, J. H., Carmichael, G. R., Newchurch, M. J., Lefer, B. L., Herman, J. R., Swap, R. J., Lau, A. K. H., Kurosu, T. P., Jaross, G., Ahlers, B., Dobber, M., McElroy, C. T., and Choi, Y.: New Era of Air Quality Monitoring from Space: Geostationary Environment Monitoring Spectrometer (GEMS), Bull. Amer. Meteorol. Soc., 101, E1-E22, 10.1175/BAMS-D-18-0013.1, 2020.

Krotkov, N. A., McLinden, C. A., Li, C., Lamsal, L. N., Celarier, E. A., Marchenko, S. V., Swartz, W. H., Bucsela, E. J., Joiner, J., Duncan, B. N., Boersma, K. F., Veefkind, J. P., Levelt, P. F., Fioletov, V. E., Dickerson, R. R., He, H., Lu, Z. F., and Streets, D. G.: Aura OMI observations of regional SO2 and NO2 pollution changes from 2005 to 2015, ATMOSPHERIC CHEMISTRY AND PHYSICS, 16, 4605-4629, 10.5194/acp-16-4605-2016, 2016.

Lamsal, L. N., Krotkov, N. A., Vasilkov, A., Marchenko, S., Qin, W., Yang, E. S., Fasnacht, Z., Joiner, J., Choi, S., Haffner, D., Swartz, W. H., Fisher, B., and Bucsela, E.: Ozone Monitoring Instrument (OMI) Aura nitrogen dioxide standard product version 4.0 with improved surface and cloud treatments, Atmos. Meas. Tech., 14, 455-479, 10.5194/amt-14-455-2021, 2021.

Laughner, J. L., and Cohen, R. C.: Direct observation of changing NO_x lifetime in North American cities, Science, 366, 723-727, doi:10.1126/science.aax6832, 2019.

Laughner, J. L., Zhu, Q., and Cohen, R. C.: Evaluation of version 3.0B of the BEHR OMI NO2 product, Atmos. Meas. Tech., 12, 129-146, 10.5194/amt-12-129-2019, 2019.

Lee, D. S., Fahey, D. W., Skowron, A., Allen, M. R., Burkhardt, U., Chen, Q., Doherty, S. J., Freeman, S., Forster, P. M., Fuglestvedt, J., Gettelman, A., De León, R. R., Lim, L. L., Lund, M. T., Millar, R. J., Owen, B., Penner, J. E., Pitari, G., Prather, M. J., Sausen, R., and Wilcox, L. J.: The contribution of global aviation to anthropogenic climate forcing for 2000 to 2018, Atmos. Environ., 244, 117834, https://doi.org/10.1016/j.atmosenv.2020.117834, 2021.

Li, C., Xu, X., Liu, X., Wang, J., Sun, K., van Geffen, J., Zhu, Q., Ma, J., Jin, J., Qin, K., He, Q., Xie, P., Ren, B., and Cohen, R. C.: Direct Retrieval of NO₂ Vertical Columns from UV-Vis (390-495 nm) Spectral Radiances Using a Neural Network, Journal of Remote Sensing, 2022, 9817134, 10.34133/2022/9817134, 2022.

Liu, H. Y., Jacob, D. J., Bey, I., and Yantosca, R. M.: Constraints from Pb-210 and Be-7 on wet deposition and transport in a global three-dimensional chemical tracer model driven by assimilated meteorological fields, J. Geophys. Res.-Atmos., 106, 12109-12128, 10.1029/2000jd900839, 2001.

Liu, M., Lin, J., Kong, H., Boersma, K. F., Eskes, H., Kanaya, Y., He, Q., Tian, X., Qin, K., Xie, P., Spurr, R., Ni, R., Yan, Y., Weng, H., and Wang, J.: A new TROPOMI product for tropospheric NO2 columns over East Asia with explicit aerosol corrections, Atmos. Meas. Tech., 13, 4247-4259, 10.5194/amt-13-4247-2020, 2020.

Lorente, A., Folkert Boersma, K., Yu, H., Dörner, S., Hilboll, A., Richter, A., Liu, M., Lamsal, L. N., Barkley, M., De Smedt, I., Van Roozendael, M., Wang, Y., Wagner, T., Beirle, S., Lin, J. T., Krotkov, N., Stammes, P., Wang, P., Eskes, H. J., and Krol, M.: Structural uncertainty in air mass factor calculation for NO2 and HCHO satellite retrievals, Atmos. Meas. Tech., 10, 759-782, 10.5194/amt-10-759-2017, 2017.

Luo, G., Yu, F., and Schwab, J.: Revised treatment of wet scavenging processes dramatically improves GEOS-Chem 12.0.0 simulations of surface nitric acid, nitrate, and ammonium over the United States, Geosci. Model Dev., 12, 3439-3447, 10.5194/gmd-12-3439-2019, 2019.

Luo, G., Yu, F., and Moch, J. M.: Further improvement of wet process treatments in GEOS-Chem v12.6.0: impact on global distributions of aerosols and aerosol precursors, Geosci. Model Dev., 13, 2879-2903, 10.5194/gmd-13-2879-2020, 2020.

Marais, E. A., Jacob, D. J., Choi, S., Joiner, J., Belmonte-Rivas, M., Cohen, R. C., Beirle, S., Murray, L. T., Schiferl, L. D., Shah, V., and Jaeglé, L.: Nitrogen oxides in the global upper troposphere: interpreting cloud-sliced NO2 observations from the OMI satellite instrument, Atmos. Chem. Phys., 18, 17017-17027, 10.5194/acp-18-17017-2018, 2018.

Marais, E. A., Roberts, J. F., Ryan, R. G., Eskes, H., Boersma, K. F., Choi, S., Joiner, J., Abuhassan, N., Redondas, A., Grutter, M., Cede, A., Gomez, L., and Navarro-Comas, M.: New observations of NO2 in the upper troposphere from TROPOMI, Atmos. Meas. Tech., 14, 2389-2408, 10.5194/amt-14-2389-2021, 2021.

Martin, R. V., Chance, K., Jacob, D. J., Kurosu, T. P., Spurr, R. J. D., Bucsela, E., Gleason, J. F., Palmer, P. I., Bey, I., Fiore, A. M., Li, Q., Yantosca, R. M., and Koelemeijer, R. B. A.: An improved retrieval of tropospheric nitrogen dioxide from GOME, Journal of Geophysical Research: Atmospheres, 107, ACH 9-1-ACH 9-21, https://doi.org/10.1029/2001JD001027, 2002.

Martin, R. V., Jacob, D. J., Chance, K., Kurosu, T. P., Palmer, P. I., and Evans, M. J.: Global inventory of nitrogen oxide emissions constrained by space-based observations of NO2 columns, Journal of Geophysical Research: Atmospheres, 108, https://doi.org/10.1029/2003JD003453, 2003.

McDuffie, E. E., Smith, S. J., O'Rourke, P., Tibrewal, K., Venkataraman, C., Marais, E. A., Zheng, B., Crippa, M., Brauer, M., and Martin, R. V.: A global anthropogenic emission inventory of atmospheric pollutants from sector- and fuel-specific sources (1970–2017): an application of the Community Emissions Data System (CEDS), Earth Syst. Sci. Data, 12, 3413-3442, 10.5194/essd-12-3413-2020, 2020.

Mebust, A. K., Russell, A. R., Hudman, R. C., Valin, L. C., and Cohen, R. C.: Characterization of wildfire NOx emissions using MODIS fire radiative power and OMI tropospheric NO2 columns, Atmos. Chem. Phys., 11, 5839-5851, 10.5194/acp-11-5839-2011, 2011.

Miyazaki, K., Eskes, H., Sudo, K., Boersma, K. F., Bowman, K., and Kanaya, Y.: Decadal changes in global surface NOx emissions from multi-constituent satellite data assimilation, Atmos. Chem. Phys., 17, 807-837, 10.5194/acp-17-807-2017, 2017.

Murray, L. T., Jacob, D. J., Logan, J. A., Hudman, R. C., and Koshak, W. J.: Optimized regional and interannual variability of lightning in a global chemical transport model constrained by LIS/OTD satellite data, Journal of Geophysical Research: Atmospheres, 117, https://doi.org/10.1029/2012JD017934, 2012.

Ott, L. E., Pickering, K. E., Stenchikov, G. L., Allen, D. J., DeCaria, A. J., Ridley, B., Lin, R. F., Lang, S., and Tao, W. K.: Production of lightning NOx and its vertical distribution calculated from three-dimensional cloud-scale chemical transport model simulations, J. Geophys. Res.-Atmos., 115, 19, 10.1029/2009jd011880, 2010.

Palm, B. B., Peng, Q., Hall, S. R., Ullmann, K., Campos, T. L., Weinheimer, A., Montzka, D., Tyndall, G., Permar, W., Hu, L., Flocke, F., Fischer, E. V., and Thornton, J. A.: Spatially Resolved Photochemistry Impacts Emissions Estimates in Fresh Wildfire Plumes, Geophys. Res. Lett., 48, e2021GL095443, https://doi.org/10.1029/2021GL095443, 2021.

Palmer, P. I., Jacob, D. J., Chance, K., Martin, R. V., Spurr, R. J. D., Kurosu, T. P., Bey, I., Yantosca, R., Fiore, A., and Li, Q.: Air mass factor formulation for spectroscopic measurements from satellites: Application to formaldehyde retrievals from the Global Ozone Monitoring Experiment, Journal of Geophysical Research: Atmospheres, 106, 14539-14550, https://doi.org/10.1029/2000JD900772, 2001.

Peng, Q. Y., Palm, B. B., Fredrickson, C. D., Lee, B. H., Hall, S. R., Ullmann, K., Campos, T., Weinheimer, A. J., Apel, E. C., Flocke, F., Permar, W., Hu, L., Garofalo, L. A., Pothier, M. A., Farmer, D. K., Ku, I. T., Sullivan, A. P., Collett, J. L., Fischer, E., and Thornton, J. A.: Observations and Modeling of NOx Photochemistry and Fate in Fresh Wildfire Plumes, Acs Earth and Space Chemistry, 5, 2652-2667, 10.1021/acsearthspacechem.1c00086, 2021.

Qu, Z., Jacob, D. J., Silvern, R. F., Shah, V., Campbell, P. C., Valin, L. C., and Murray, L. T.: US COVID-19 Shutdown Demonstrates Importance of Background NO2 in Inferring NOx Emissions From Satellite NO2 Observations, Geophys. Res. Lett., 48, e2021GL092783, https://doi.org/10.1029/2021GL092783, 2021.
Reed, C., Evans, M. J., Crilley, L. R., Bloss, W. J., Sherwen, T., Read, K. A., Lee, J. D., and Carpenter, L. J.: Evidence for renoxification in the tropical marine boundary layer, Atmos. Chem. Phys., 17, 4081-4092, 10.5194/acp-17-4081-2017, 2017.
Richards, N. K., Wingen, L. M., Callahan, K. M., Nishino, N., Kleinman, M. T., Tobias, D. J., and Finlayson-Pitts, B. J.: Nitrate Ion Photolysis in Thin Water Films in the Presence of Bromide Ions, The Journal of Physical Chemistry A, 115, 5810-5821, 10.1021/jp109560j, 2011.
Richards, N. K., Anderson, C., Anastasio, C., and Finlayson-Pitts, B. J.: The effect of cations on NO2 production from the photolysis of aqueous thin water films of nitrate salts, Physical Chemistry Chemical Physics, 17, 32211-32218, 10.1039/C5CP05325K, 2015.
Rolph, G. D., Draxler, R. R., Stein, A. F., Taylor, A., Ruminski, M. G., Kondragunta, S., Zeng, J., Huang, H.-C., Manikin, G., McQueen, J. T., and Davidson, P. M.: Description and Verification of the NOAA Smoke Forecasting System: The 2007 Fire Season, Weather and Forecasting, 24, 361-378, 10.1175/2008waf2222165.1, 2009.
Russell, A. R., Valin, L. C., and Cohen, R. C.: Trends in OMI NO2 observations over the United States: effects of emission control technology and the economic recession, Atmos. Chem. Phys., 12, 12197-12209, 10.5194/acp-12-12197-2012, 2012.
Scharko, N. K., Berke, A. E., and Raff, J. D.: Release of Nitrous Acid and Nitrogen Dioxide from Nitrate Photolysis in Acidic Aqueous Solutions, Environ. Sci. Technol., 48, 11991-12001, 10.1021/es503088x, 2014.
Shah, V., Jacob, D. J., Dang, R., Lamsal, L. N., Strode, S. A., Steenrod, S. D., Boersma, K. F., Eastham, S. D., Fritz, T. M., Thompson, C., Peischl, J., Bourgeois, I., Pollack, I. B., Nault, B. A., Cohen, R. C., Campuzano-Jost, P., Jimenez, J. L., Andersen, S. T., Carpenter, L. J., Sherwen, T., and Evans, M. J.: Nitrogen oxides in the free troposphere: implications for tropospheric oxidants and the interpretation of satellite NO2 measurements, Atmos. Chem. Phys., 23, 1227-1257, 10.5194/acp-23-1227-2023, 2023.
Silvern, R. F., Jacob, D. J., Travis, K. R., Sherwen, T., Evans, M. J., Cohen, R. C., Laughner, J. L., Hall, S. R., Ullmann, K., Crounse, J. D., Wennberg, P. O., Peischl, J., and Pollack, I. B.: Observed NO/NO2 Ratios in the Upper Troposphere Imply Errors in NO-NO2-O3 Cycling Kinetics or an Unaccounted NOx Reservoir, Geophys. Res. Lett., 45, 4466-4474, https://doi.org/10.1029/2018GL077728, 2018.
Silvern, R. F., Jacob, D. J., Mickley, L. J., Sulprizio, M. P., Travis, K. R., Marais, E. A., Cohen, R. C., Laughner, J. L., Choi, S., Joiner, J., and Lamsal, L. N.: Using satellite observations of tropospheric NO2 columns to infer long-term trends in US NOx emissions: the importance of accounting for the free tropospheric NO2 background, Atmos. Chem. Phys., 19, 8863-8878, 10.5194/acp-19-8863-2019, 2019.
Simone, N. W., Stettler, M. E. J., and Barrett, S. R. H.: Rapid estimation of global civil aviation emissions with uncertainty quantification, Transportation Research Part D: Transport and Environment, 25, 33-41, https://doi.org/10.1016/j.trd.2013.07.001, 2013.
Travis, K. R., Jacob, D. J., Fisher, J. A., Kim, P. S., Marais, E. A., Zhu, L., Yu, K., Miller, C. C., Yantosca, R. M., Sulprizio, M. P., Thompson, A. M., Wennberg, P. O., Crounse, J. D., St. Clair, J. M., Cohen, R. C., Laughner, J. L., Dibb, J. E., Hall, S. R., Ullmann, K., Wolfe, G. M., Pollack, I. B., Peischl, J., Neuman, J. A., and Zhou, X.: Why do models overestimate surface ozone in the Southeast United States?, Atmos. Chem. Phys., 16, 13561-13577, 10.5194/acp-16-13561-2016, 2016.
Travis, K. R., Heald, C. L., Allen, H. M., Apel, E. C., Arnold, S. R., Blake, D. R., Brune, W. H., Chen, X., Commane, R., Crounse, J. D., Daube, B. C., Diskin, G. S., Elkins, J. W., Evans, M. J., Hall, S. R., Hintsa, E. J., Hornbrook, R. S., Kasibhatla, P. S., Kim, M. J., Luo, G., McKain, K., Millet, D. B., Moore, F. L., Peischl, J., Ryerson, T. B., Sherwen, T., Thames, A. B., Ullmann, K., Wang, X., Wennberg, P. O., Wolfe, G. M., and Yu, F.: Constraining remote oxidation capacity with ATom observations, Atmos. Chem. Phys., 20, 7753-7781, 10.5194/acp-20-7753-2020, 2020.
van der Werf, G. R., Randerson, J. T., Giglio, L., van Leeuwen, T. T., Chen, Y., Rogers, B. M., Mu, M., van Marle, M. J. E., Morton, D. C., Collatz, G. J., Yokelson, R. J., and Kasibhatla, P. S.: Global fire emissions estimates during 1997–2016, Earth Syst. Sci. Data, 9, 697-720, 10.5194/essd-9-697-2017, 2017.
van Geffen, J., Boersma, K. F., Eskesl, H., Sneep, M., ter Linden, M., Zara, M., and Veefkind, J. P.: S5P TROPOMI NO2 slant column retrieval: method, stability, uncertainties and comparisons with OMI, Atmos. Meas. Tech., 13, 1315-1335, 10.5194/amt-13-1315-2020, 2020.
Vasilkov, A., Krotkov, N., Yang, E. S., Lamsal, L., Joiner, J., Castellanos, P., Fasnacht, Z., and Spurr, R.: Explicit and consistent aerosol correction for visible wavelength satellite cloud and nitrogen dioxide retrievals based on optical properties from a global aerosol analysis, Atmos. Meas. Tech., 14, 2857-2871, 10.5194/amt-14-2857-2021, 2021.
Vinken, G. C. M., Boersma, K. F., Maasakkers, J. D., Adon, M., and Martin, R. V.: Worldwide biogenic soil NOx emissions inferred from OMI NOx observations, Atmos. Chem. Phys., 14, 10363-10381, 10.5194/acp-14-10363-2014, 2014.
Wang, X., Dalton, E. Z., Payne, Z. C., Perrier, S., Riva, M., Raff, J. D., and George, C.: Superoxide and Nitrous Acid Production from Nitrate Photolysis Is Enhanced by Dissolved Aliphatic Organic Matter, Environ. Sci. Technol. Lett., 8, 53-58, 10.1021/acs.estlett.0c00806, 2021.
Wang, X., Jacob, D. J., Downs, W., Zhai, S., Zhu, L., Shah, V., Holmes, C. D., Sherwen, T., Alexander, B., Evans, M. J., Eastham, S. D., Neuman, J. A., Veres, P. R., Koenig, T. K., Volkamer, R., Huey, L. G., Bannan, T. J., Percival, C. J., Lee, B. H., and Thornton, J. A.: Global tropospheric halogen (Cl, Br, I) chemistry and its impact on oxidants, Atmos. Chem. Phys., 21, 13973-13996, 10.5194/acp-21-13973-2021, 2021.

Wang, Y., Wang, J., Xu, X., Henze, D. K., Qu, Z., and Yang, K.: Inverse modeling of SO2 and NOx emissions over China using multisensor satellite data – Part 1: Formulation and sensitivity analysis, Atmos. Chem. Phys., 20, 6631-6650, 10.5194/acp-20-6631-2020, 2020.
Wang, Y., Ge, C., Castro Garcia, L., Jenerette, G. D., Oikawa, P. Y., and Wang, J.: Improved modelling of soil NOx emissions in a high temperature agricultural region: role of background emissions on NO2 trend over the US, Environ. Res. Lett., 16, 084061, 10.1088/1748-9326/ac16a3, 2021.
Wesely, M. L.: PARAMETERIZATION OF SURFACE RESISTANCES TO GASEOUS DRY DEPOSITION IN REGIONAL-SCALE NUMERICAL-MODELS, Atmos. Environ., 23, 1293-1304, 10.1016/0004-6981(89)90153-4, 1989.
Westerling, A. L.: Increasing western US forest wildfire activity: sensitivity to changes in the timing of spring, Philosophical Transactions of the Royal Society B: Biological Sciences, 371, 20150178, 10.1098/rstb.2015.0178, 2016.
Wilkerson, J. T., Jacobson, M. Z., Malwitz, A., Balasubramanian, S., Wayson, R., Fleming, G., Naiman, A. D., and Lele, S. K.: Analysis of emission data from global commercial aviation: 2004 and 2006, Atmos. Chem. Phys., 10, 6391-6408, 10.5194/acp-10-6391-2010, 2010.
Wingen, L. M., Moskun, A. C., Johnson, S. N., Thomas, J. L., Roeselová, M., Tobias, D. J., Kleinman, M. T., and Finlayson-Pitts, B. J.: Enhanced surface photochemistry in chloride–nitrate ion mixtures, Physical Chemistry Chemical Physics, 10, 5668-5677, 10.1039/B806613B, 2008.
Yang, K., Carn, S. A., Ge, C., Wang, J., and Dickerson, R. R.: Advancing measurements of tropospheric NO2 from space: New algorithm and first global results from OMPS, Geophys. Res. Lett., 41, 4777-4786, https://doi.org/10.1002/2014GL060136, 2014.
Ye, C., Zhou, X., Pu, D., Stutz, J., Festa, J., Spolaor, M., Tsai, C., Cantrell, C., Mauldin, R. L., Campos, T., Weinheimer, A., Hornbrook, R. S., Apel, E. C., Guenther, A., Kaser, L., Yuan, B., Karl, T., Haggerty, J., Hall, S., Ullmann, K., Smith, J. N., Ortega, J., and Knote, C.: Rapid cycling of reactive nitrogen in the marine boundary layer, Nature, 532, 489-491, 10.1038/nature17195, 2016.
Ye, C., Zhang, N., Gao, H., and Zhou, X.: Photolysis of Particulate Nitrate as a Source of HONO and NOx, Environ. Sci. Technol., 51, 6849-6856, 10.1021/acs.est.7b00387, 2017.
Zhai, S., Jacob, D. J., Wang, X., Liu, Z., Wen, T., Shah, V., Li, K., Moch, J. M., Bates, K. H., Song, S., Shen, L., Zhang, Y., Luo, G., Yu, F., Sun, Y., Wang, L., Qi, M., Tao, J., Gui, K., Xu, H., Zhang, Q., Zhao, T., Wang, Y., Lee, H. C., Choi, H., and Liao, H.: Control of particulate nitrate air pollution in China, Nat. Geosci., 14, 389-395, 10.1038/s41561-021-00726-z, 2021.
Zhang, J., Zhang, S., Zhang, X., Wang, J., Wu, Y., and Hao, J.: Developing a High-Resolution Emission Inventory of China's Aviation Sector Using Real-World Flight Trajectory Data, Environ. Sci. Technol., 10.1021/acs.est.1c08741, 2022.
Zhang, R., Gen, M., Huang, D., Li, Y., and Chan, C. K.: Enhanced Sulfate Production by Nitrate Photolysis in the Presence of Halide Ions in Atmospheric Particles, Environ. Sci. Technol., 54, 3831-3839, 10.1021/acs.est.9b06445, 2020.
Zhu, L., Val Martin, M., Gatti, L. V., Kahn, R., Hecobian, A., and Fischer, E. V.: Development and implementation of a new biomass burning emissions injection height scheme (BBEIH v1.0) for the GEOS-Chem model (v9-01-01), Geosci. Model Dev., 11, 4103-4116, 10.5194/gmd-11-4103-2018, 2018.
Zhu, Q., Laughner, J. L., and Cohen, R. C.: Lightning NO2 simulation over the contiguous US and its effects on satellite NO2 retrievals, Atmos. Chem. Phys., 19, 13067-13078, 10.5194/acp-19-13067-2019, 2019.